BIOCHEMISTRY
including biophysical chemistry & molecular biology

Article

pubs.acs.org/biochemistry

Delineation of Solution Burst-Phase Protein Folding Events by Encapsulating the Proteins in Silica Gels

Takahiro Okabe,[†] Seiichi Tsukamoto,[†,§] Kazuo Fujiwara,[†] Naoya Shibayama,[‡] and Masamichi Ikeguchi*[,†]

[†]Department of Bioinformatics, Soka University, 1-236 Tangi-machi, Hachioji, Tokyo 192-8577, Japan

[‡]Department of Physiology, Division of Biophysics, Jichi Medical University, 3311-1 Yakushiji, Shimotsuke, Tochigi 329-0498, Japan

ABSTRACT: Many studies have shown that during the early stages of the folding of a protein, chain collapse and secondary structure formation lead to a partially folded intermediate. Thus, direct observation of these early folding events is crucial if we are to understand protein-folding mechanisms. Notably, these events usually manifest as the initial unresolvable signals, denoted the burst phase, when monitored during conventional mixing experiments. However, folding events can be substantially slowed by first trapping a protein within a silica gel with a large water content, in which the trapped native state retains its solution conformation. In this study, we monitored the early folding events involving secondary structure formation of five globular proteins, horse heart cytochrome *c*, equine *β*-lactoglobulin, human tear lipocalin, bovine *α*-lactalbumin, and hen egg lysozyme, in silica gels containing 80% (w/w) water by CD spectroscopy. The folding rates decreased for each of the proteins, which allowed for direct observation of the initial folding transitions, equivalent to the solution burst phase. The formation of each initial intermediate state exhibited single exponential kinetics and Arrhenius activation energies of 14−31 kJ/mol.

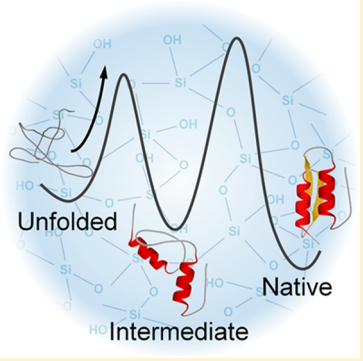

There is increasing evidence that the initial step(s) in the folding of a protein (within microseconds to milliseconds) involves chain collapse and secondary structure formation.[1−5] Rapid mixing techniques in conjunction with spectroscopic probes are commonly used to explore folding reactions that occur within the aforementioned time range. However, such techniques cannot readily differentiate among early folding events because of time-resolution limits. For many proteins, the burst phase, which has often been interpreted as the rapid formation of an intermediate (I) state, occurs within the dead time of the mixing apparatus. Although recent development of several laser-based methods has made it possible to monitor folding on the nanosecond to microsecond time scale, these fast methods are limited to certain types of proteins and experimental systems.[6,7] Thus, there are several fundamental questions about early folding events that, while having received considerable attention from experimentalists and theorists, remain unresolved. Such questions include the following: For a given protein, is the burst phase a single-step or multistep process? Do chain collapse and secondary structure formation occur simultaneously or sequentially? Is formation of an I state a barrier-crossing or barrier-less transition? To improve our understanding of early folding transitions, direct observation of such events is required.

Within a porous silica gel with a large water content, large-scale protein motions are dramatically slowed, although the in-gel native (N) state can retain its solution properties.[8−11] In particular, the folding of a protein in such a gel is dramatically slowed, which makes it possible to directly observe the entire folding process without substantially perturbing its folding pathway.[12−15] However, the physical mechanism responsible for the deceleration is not well understood. One possibility involves an indirect water-mediated interaction with the protein[16] since the water-molecule dynamics in the silica pores are very different from those of bulk water and could influence protein dynamics.[17,18]

Previously, one of us (N.S.) applied the gel method to probe the folding of oxidized horse cytochrome *c* (CYT), bovine ubiquitin, and bovine *β*-lactoglobulin (BLG).[14,15] For CYT, a collapse leading to the I state corresponding to the burst-phase intermediate in solution was observed. Moreover, the folding kinetics of its I state could be fit to a stretched exponential function, a signature of a barrier-less process.[19] For BLG, the I state similar to the burst-phase intermediate in solution was formed via the earliest observable transition.[15] However, in contrast to early folding of CYT, the earliest observable transition for BLG exhibits a single exponential decay, a signature of a barrier-limited process.[19]

For the study reported herein, to gain more insight into early folding events, we extended the gel entrapment method to two pairs of homologous proteins. One pair is equine *β*-lactoglobulin (ELG) and human tear lipocalin (HTL), both of which belong to the lipocalin family and have an eight-stranded up-and-down *β*-barrel fold (Figure 1). As with BLG, ELG forms non-native helical structures during its burst phase;[20] however, the non-native helical structures in the two proteins do not appear in the same location.[21,22] Conversely, HTL does not form burst-phase non-native helical structures.[23] Because the CD amplitude of the burst-phase change is small, it

Received: March 26, 2014
Revised: May 23, 2014
Published: May 27, 2014

   dx.doi.org/10.1021/bi5003647 | *Biochemistry* 2014, 53, 3858−3866

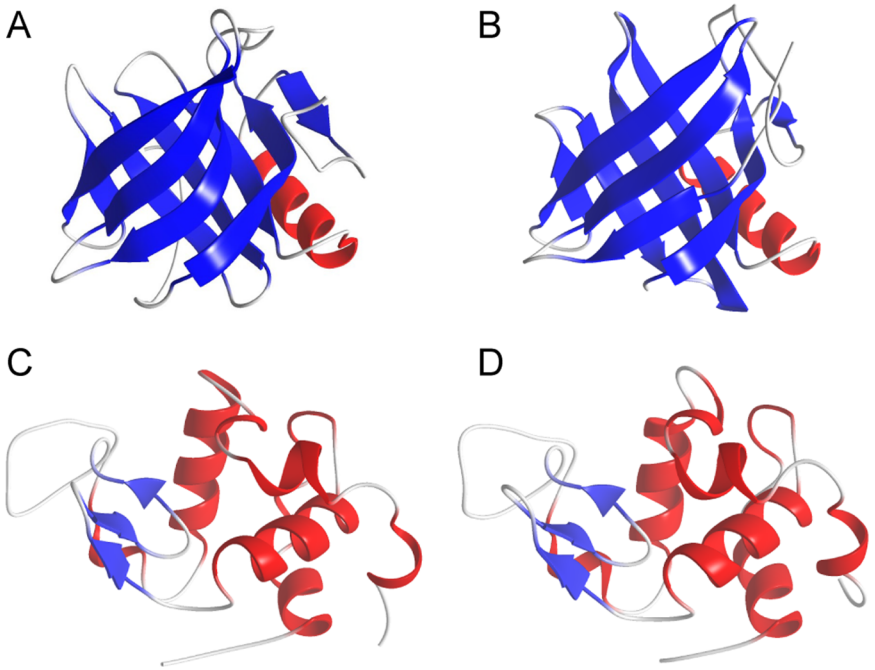

Figure 1. Three-dimensional structures of (A) β-lactoglobulin (PDB ID, 3NPO), (B) tear lipocalin (PDB ID, 3EYC), (C) α-lactalbumin (PDB ID, 1HFZ), and (D) lysozyme (PDB ID, 3A8Z).

can be argued that the burst-phase change in the CD signal of HTL reflects the collapse of the unfolded protein upon dilution of the denaturant instead of formation of discrete I states. Bovine α-lactalbumin (BLA) and hen egg white lysozyme (LYZ) form the second homologous pair. They belong to the c-type lysozyme family, and their common fold contains an α-domain (four α-helices and one 3_{10}-helix) and a β-domain (a triple-stranded, antiparallel β-sheet, a 3_{10}-helix, and a long loop; Figure 1). The folding mechanisms for these two proteins have been extensively studied, and the structures of their burst-phase folding I states and equilibrium analogues are well characterized.[24−31] For this study, we asked whether the burst-phase transitions for these four proteins occur in a single step or in multiple steps, whether their burst-phase events are barrier-crossing or barrier-less reactions, and, if any, what are the heights of energy barriers?

MATERIALS AND METHODS

Protein Samples. CYT and LYZ were purchased from Sigma and Seikagaku Kogyo Corporation, Ltd., respectively, and used without further purification. ELG and BLA were purified from equine and bovine milk, respectively.[32] HTL is a mutant of human tear lipocalin, in which Cys101 is replaced with an alanine to prevent thiol−disulfide exchange during unfolding and folding. It was expressed in *Escherichia coli* and purified as described.[23] Protein purities were confirmed by SDS-PAGE and analytical reverse-phase HPLC.

Entrapment of Proteins in Silica Gels. Gels were prepared as described[14] with modifications. Tetramethylorthosilicate (TMOS) was purchased from Tokyo Kasei. Equal volumes of TMOS and 2 mM HCl were mixed and sonicated in an ice/water bath for 40 min to form $Si(OH)_4$. Next, 100 μL of the resultant silica sol was mixed with 150 μL of an ice-cold 0.5 mM protein solution in 0.2 M potassium phosphate, pH 7.1. After the solution had been mixed, 75 μL of the mixture was immediately coated onto a framed quartz plate (10 mm × 40 mm × 0.1 mm; TOSOH Quartz) pretreated with 4 M KOH for 30 min to maximize the number of surface silanol groups. A Teflon plate was placed over the sample to form a 0.1 mm thick gel (Figure 2A). Gelation occurred within 1 min at room temperature. The samples were aged at 25 °C for 2 h (ELG, HTL, and BLA) or 6 h (LYZ and CYT). Next, the Teflon plate was removed, and the silica gel, while still attached to its quartz plate, was soaked in distilled water to finish the aging process. The concentrations of the proteins within the gels were spectrophotometrically determined. To confirm that the trapped proteins retain their N states in the gels, the gels were soaked in folding buffer, after which their CD spectra were recorded.

Refolding Experiments. Before the folding procedure was started, each silica gel on its quartz plate was immersed into 6.0 M guanidine hydrochloride (GdnHCl), 0.2 M potassium phosphate, pH 4.2 (ELG); 6.0 M GdnHCl, 0.2 M potassium phosphate, pH 7.0 (HTL and BLA); 6.0 M GdnHCl, 0.2 M phosphoric acid, pH 1.8 (LYZ); or 0.2 M phosphoric acid, pH 1.8 (CYT) for 5 min at 25 °C. To measure the early folding kinetics (5−300 s), the quartz plate/gel/unfolded protein system was attached onto the open side a custom-made, rectangular three-sided quartz cuvette (1 cm path length; Sakamoto Kougaku, (Tokyo)) (Figure 2B). The folding reactions were initiated by injection of 3.6 mL of 1 M potassium phosphate, pH 4.2 (ELG); 0.2 M potassium phosphate, pH 7.0 (HTL and BLA); 0.2 M phosphoric acid, pH 1.8 (LYZ); or 0.5 M potassium phosphate, pH 4.5 (CYT) into the cuvette. The solution in the cuvette was mixed by pipetting up and down several times. For spectral measurements made at >180 s, each system was simply immersed into the appropriate folding buffer for 150 s and then covered with a quartz plate to prevent protein leakage and drying during the measurements (Figure 2C).

Folding Dead Time. To determine the diffusion time needed to reduce the GdnHCl concentration inside the gels

dx.doi.org/10.1021/bi5003647 | *Biochemistry* 2014, 53, 3858−3866

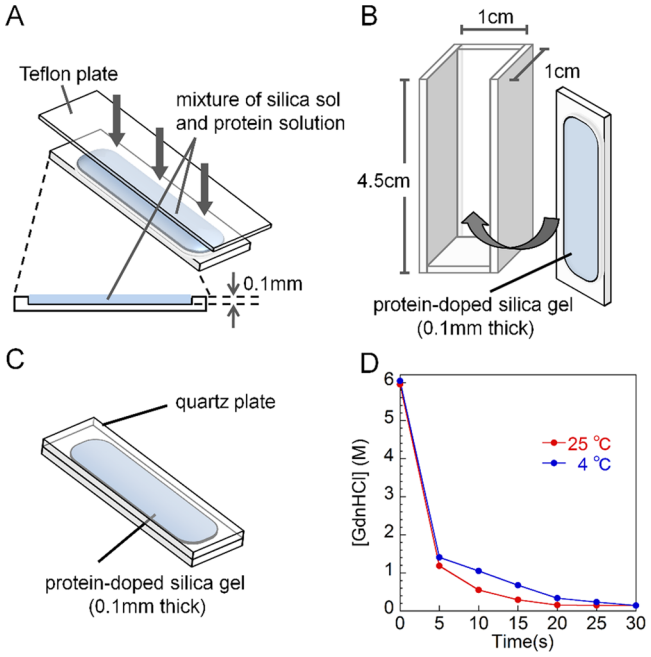

Figure 2. Illustration of optical cell assembly. (A) A silica gel film was prepared on a framed quartz plate (10 mm × 40 mm × 0.1 mm). A Teflon plate was placed over the sample to form a 0.1 mm thick gel. (B) The custom-made, three-sided quartz cuvette and a protein doped silica gel adhering to the quartz plate are assembled to form a 1 cm path length cuvette. This cell was used to follow the time course within 300 s. (C) In the case of spectral measurements after 180 s, the silica gel film on a framed quartz plate was immersed into the appropriate folding buffer for 150 s and then covered with a quartz plate to prevent protein leakage and drying during the measurements. (D) The diffusion of GdnHCl from inside the 0.1 mm thick gel at 25 and 4 °C followed by the absorbance at 207.5 nm.

after injection of a refolding buffer, we performed the previously reported control experiment: a protein-free gel of 0.1 mm thickness was equilibrated with 6.0 M GdnHCl. Then, the cuvette was assembled as shown Figure 2B, and 3.6 mL of 0.5 M potassium phosphate (pH 4.5) was injected into the cuvette. The pipetting for mixing was done during the first 5 s. After a given time, we threw away the buffer in the cuvette and measured the absorbance of the gel ($A_{207.5}$), from which GdnHCl concentration was estimated (Figure 2D). The GdnHCl diffusion within 5 s did not significantly vary between 5 and 25 °C or with the aging time probably because the mixing by pipetting is effective. After 5 s, diffusion seems to be temperature-dependent. Although 20−30 s was required to reach the equilibrium value of the GdnHCl concentration, we monitored each folding reaction starting at 5 s after the buffer injection because the rate constant of the fastest folding phase was shown to be insensitive to the GdnHCl concentration.[33]

CD Spectroscopy. CD spectra were recorded using Jasco J-720 and Applied Photophysics Chirascan spectropolarimeters equipped with a Peltier element for temperature control. For the kinetic studies, the mean residue ellipticity (MRE) of a given wavelength was recorded every 0.5 s with a 2 nm bandwidth. CD spectra from 200 to 250 nm were collected every 0.2 nm with a 2 nm bandwidth.

RESULTS

Optimization of Encapsulation Conditions. Previously, CYT, ubiquitin, and BLG have been successfully encapsulated in the silica gels (~70% (w/w) water) keeping their N-state conformations.[14,15] Although the same procedure was applied for proteins used in this study, the CD spectra of HTL and BLA trapped in gels indicate that they are partially unfolded. To reduce the concentration of methanol that is produced by hydrolysis of TMOS and destabilizes proteins, we decreased TMOS content (increased the water content). When the water content is increased to ~80% (w/w), each in-gel protein maintains its N state and the gels remain optically transparent and mechanically stable. Because the silica network is strengthen when aged,[14] the conformational constraints on a trapped protein and thus on its folding rates can be controlled by varying the aging time. We thus chose an aging time for each

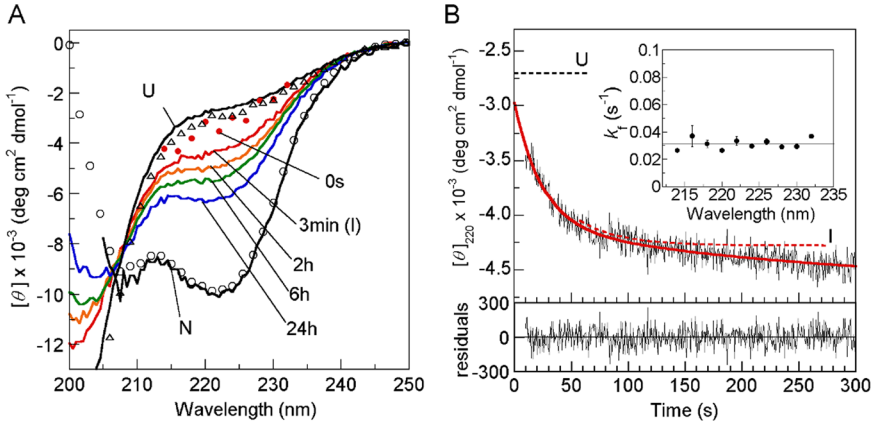

Figure 3. (A) Representative far-UV CD spectra recorded during the folding of CYT at 25 °C and pH 4.5 in a silica gel containing 80% (w/w) water. The times indicated are those after initiation of the folding reaction. The red circles correspond to the mean residue ellipticities (MREs) obtained by extrapolation of kinetic curves to time zero. The solid black lines represent the spectra of the N and U states in gel. The open circles and triangles are the MREs of the spectra of the N and U states, respectively, in solution. Note that the spectra of the solution N and U states were recorded using the same folding and unfolding conditions as were used for the gel measurements. (B) Representative kinetic curve plotted using the MRE at 220 nm for the initial resolvable CYT in-gel folding phase at 25 °C. The times are those after initiation of the folding reaction. The thick red line is the fitted curve drawn using eq 1 and $\beta = 1$. The dotted red curve is the single exponential curve. The dotted black line in the upper panel is the MRE at 220 nm for the U state. The residuals are shown in the lower panel. The inset shows the folding rate constants calculated for each wavelength. The horizontal line is the average value of the rate constant.

dx.doi.org/10.1021/bi5003647 | Biochemistry 2014, 53, 3858−3866

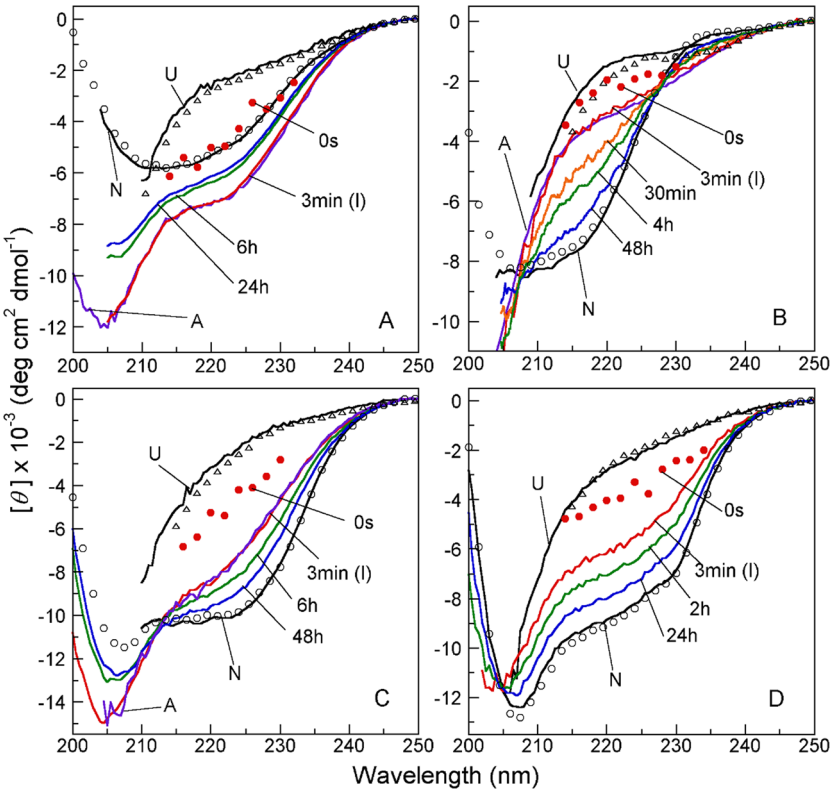

Figure 4. Representative far-UV CD spectra recorded during the folding of (A) ELG, (B) HTL, (C) BLA, and (D) LYZ at 25 °C each in a silica gel containing 80% (w/w) water. The times indicated are those after initiation of the folding reaction. The red circles correspond to MREs obtained by extrapolation of kinetic curves to time zero. The solid black lines represent the spectra of the N and U states in gel. The open circles and triangles represent the CD spectra of the solution N and U states, respectively. Note that the spectra of the solution N and U states were measured under the conditions used for the gel measurements. In panels A, B, and C, the purple lines, which coincide with the spectra taken at 3 min, are the CD spectra for the acid-denatured (A) states in gels equilibrated with 0.2 M phosphoric acid, pH 1.8.

protein that would prevent its leakage from a gel and that would decelerate its burst-phase folding events, which would allow the folding kinetics to be followed spectroscopically.

To confirm that the change in the gel conditions did not affect our results, we reinvestigated the folding of CYT (Figure 3). The CD spectrum of native CYT in the gel is identical to its solution spectrum (Figure 3A), indicating that the native conformation is maintained in the gel. Folding of CYT was initiated from its acid-unfolded state (pH 1.8). The CD spectra of the unfolded (U) states in solution and in the gel at pH 1.8 are nearly identical (Figure 3A), indicating that the CYT U state is also not influenced by the gel matrix. As shown previously,[14] in-gel folding of CYT is slowed substantially such that the native CD spectrum is only 50% recovered by 24 h (Figure 3A). Figure 3B shows a representative kinetic folding curve monitored by CD at 220 nm for 300 s. The plot exhibits two distinct phases. The rate constants were determined by fitting the following equation:

$$[\theta](t) = [\theta]_\infty - [\theta]_f \exp\{-(k_f t)^\beta\} - [\theta]_s \exp\{-(k_s t)\} \quad (1)$$

where $[\theta]_\infty$, $[\theta]_f$, and $[\theta]_s$ are the equilibrium, fast-phase, and slow-phase MREs at a given wavelength, respectively. The parameters k_f, k_s, and β are the rate constants for the fast and slow phases and the stretching factor, respectively. The stretching factor is ~1 for the curve shown in Figure 3B; we, therefore, used $\beta = 1$ for the following analysis. The fast-phase CYT rate constants are independent of the observed wavelengths (Figure 3B, inset) and reflect the appearance of the CD spectrum of the species I shown in Figure 3A. The CD spectrum of the I state, acquired within 3 min (Figure 3A), is similar to the spectrum recorded at 2 min previously for CYT trapped in a gel containing 70% (w/w) water and a 4-h aging time (see Figure 1A in ref 14). The MRE values at each wavelength when extrapolated back to zero time did not coincide with the values of the U state, which indicates the earlier burst-phase event occurred in the gel. Thus, we obtained essentially identical results in both studies even though the water content of the gels differed. The previous absorption and fluorescence study showed that the in-gel burst phase of CYT is coordination of proximal His18 to the heme and the I state is a partially collapsed state.[14]

For the other four proteins, the far-UV CD spectra of their N states in the gels are nearly identical to their corresponding solution spectra (Figure 4), indicating that the gel environment did not perturb their secondary structures. Furthermore, the CD spectra of the in-gel proteins under unfolding conditions are similar to the corresponding solution spectra, indicating that the gel environment also did not affect their U states.

Folding in the Gel. Folding of each protein was initiated by immersing a protein-containing gel into one of the folding solutions described in Materials and Methods. Water and chemical solute diffusion was much more rapid than the folding reactions themselves (see Materials and Methods). Representative CD spectral snapshots during folding of each in-gel protein are shown in Figure 4. In all cases, the spectra gradually shift from that of the corresponding U state to that of the

dx.doi.org/10.1021/bi5003647 | Biochemistry 2014, 53, 3858−3866

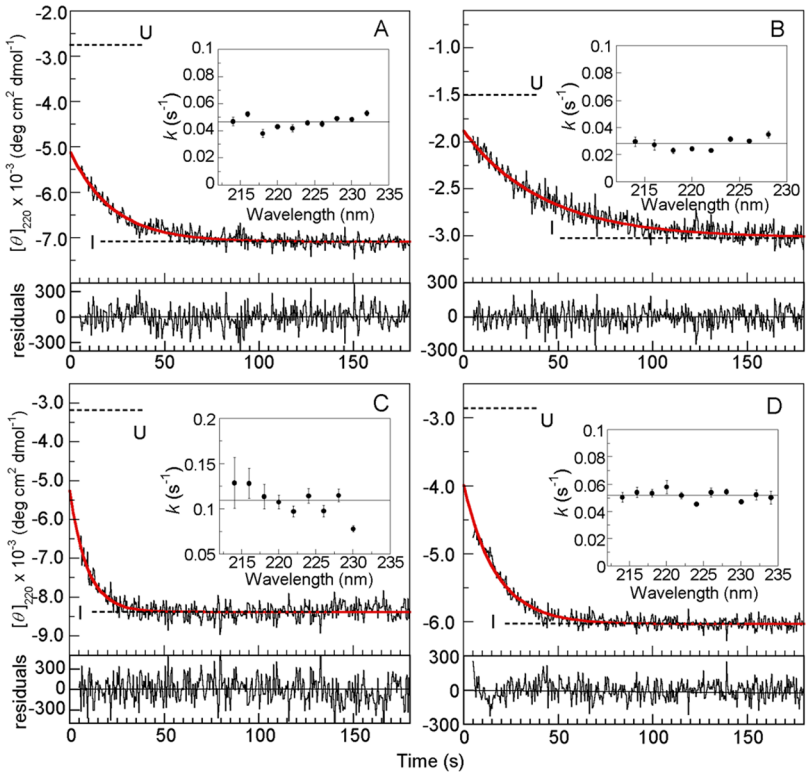

Figure 5. Representative plots of the MRE at 220 nm during the U → I transitions at 25 °C for (A) ELG, (B) HTL, (C) BLA, and (D) LYZ in the gels. The times are those after initiation of the folding reaction. The thick red lines are each a fit to a single exponential. The dotted lines are the MRE values for the U and I states at 220 nm. The residuals are shown under each kinetic plot. The insets show the refolding rate constants calculated for each wavelength, with the horizontal lines being the average values.

corresponding N state, albeit 4−6 orders of magnitude slower than would occur in solution.

Early ELG Folding. The secondary structure of native ELG is mainly a β-sheet (Figure 1). Nevertheless, CD spectroscopy used in conjunction with a stopped-flow apparatus has shown that a solution burst-phase state accumulates within the dead time of the measurement with a far-UV CD spectrum that is more negative overall than is that of the N state, suggesting that non-native helical structures form.[20] ELG can also form an equilibrium molten globule at acid pH (the A state),[34] which is equivalent to the solution burst-phase I state.[20]

We initiated in-gel folding of ELG by a GdnHCl concentration jump from 6 to 0 M. As observed for folding of ELG in solution, its spectrum recorded prior to complete folding is more negative than its N-state spectrum (Figure 4A). At times longer than 3 min of folding, the MRE values of the in-gel ELG spectra slowly increased. Figure 5A shows a representative folding curve for in-gel ELG monitored at 220 nm. The extended folding time of in-gel ELG allowed us to observe the folding kinetics leading to an I state. Because the decay curve plateaued at 3 min, the corresponding spectrum can be regarded as identical to that of the in-gel I state (Figure 4A). The CD spectra of the kinetic I state and in-gel equilibrium A state are similar in shape and amplitude to those of the solution burst-phase I and A states, which strongly suggests that the in-gel I state corresponds to the solution burst-phase I state. To obtain detailed kinetic information concerning the earliest observable stage of ELG folding, we monitored the changes in the MRE of its spectrum between 212 and 232 nm from 5 to 180 s. The curves acquired at the various wavelengths were fit with virtually the same single exponential function; that is, the extracted rate constants have identical values (Figure 5A inset), strongly suggesting that the curves all report the same process. The MRE values at each wavelength when extrapolated back to zero time do not coincide with the corresponding values of the U state, which indicates that an earlier burst-phase event occurred in the gel. This transition is discussed below in more detail.

Early HTL Folding. Although HTL is structurally homologous to ELG, its folding in solution differs.[23] In contrast to ELG folding, non-native helix formation is absent during HTL folding. The MRE value for the solution HTL burst phase is less and more negative than that of its U state at 230 and 215 nm, respectively.[23] This spectral characteristic is similar to that of the N state, which suggests that the solution burst-phase I state contains a partial native-like β-structure. The difference in the structures of the burst-phase HTL and ELG species has been ascribed to the difference in the helical propensities of their amino acid sequences.[23] The non-native helical structures in the solution ELG I state appear to be largely stabilized by the disulfide formed by residues Cys106 and Cys119, which is absent in HTL.[35] HTL can also be acid denatured to an equilibrium A state; however, the CD spectrum of its solution A state is different from that of the solution burst-phase I state.[23]

The CD spectra acquired during the folding of in-gel HTL and a kinetic curve recorded at 220 nm are shown in Figures 4B and 5B, respectively. The folding curves acquired by monitoring the MRE values at various wavelengths could be fit with a single exponential function and with identical rate constants (Figure 5B inset). Therefore, the folding curves all reflect the same process, that is, formation of an I state. Although the types of secondary structures contained in the I

dx.doi.org/10.1021/bi5003647 | *Biochemistry* 2014, 53, 3858−3866

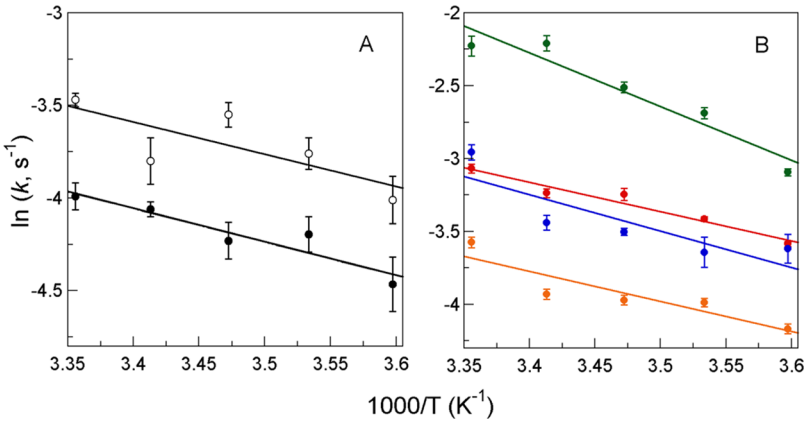

Figure 6. (A) Arrhenius plots of the I-state formation rates of CYT in gels aged for 6 h (open circles) or 48 h (closed circles). (B) Arrhenius plots of the I-state formation rates of ELG (red), HTL (orange), BLA (green), and LYZ (blue). In both panels, the straight lines are linear fits to the data. The corresponding activation energies are listed in Table 1.

state are not obvious from its CD spectrum (the 3 min spectrum, Figure 4B), the fact that the transition to the I state involves an exponential relaxation process suggests that the I and U states are discrete states. Notably, the spectrum of the in-gel I state is identical to that of the in-gel A state but is different from the solution burst-phase I state. That is, the A state appears as a kinetic intermediate in gel although it does not appear during folding in solution. The in-gel I state (A state) may be an intermediate preceding to the solution I state, and its appearance could not resolved in the previous solution study. Alternatively, the solution I state, which is more stable than the solution A state, may be unstable in gel. Further studies are required to clarify the relationship between the in-gel I state and the solution I state of HTL.

Early BLA Folding. The solution burst-phase I state of BLA was found ~30 years ago[24] and is equivalent to the BLA A state observed at acid pH or in solutions containing moderate concentrations of denaturants.[25] The structures of the solution BLA kinetic I and equilibrium A states have been well characterized.[28−31] It seems to contain an N-like cleft region, which includes an organized C-helix.[28,30]

Spectral snapshots and a kinetic curve for in-gel BLA folding are shown in Figures 4C and 5C, respectively. The folding curves acquired at various wavelengths were fit with a single exponential function and with identical rate constants (Figure 5C, inset). The spectrum of the BLA I state (the 3 min spectrum, Figure 4C) is identical to that of the in-gel equilibrium A state like the spectrum of the solution I state is identical to that of the solution A state. Additionally, the CD spectra of the in-gel I and A states closely resemble the corresponding solution I- and A-state spectra.[24]

Early LYZ Folding. The folding mechanism of LYZ has been extensively investigated using a variety of techniques including hydrogen/deuterium-exchange labeling combined with NMR or mass spectrometry.[26,27] During the dead time of the stopped-flow apparatus (<2 ms), CD spectroscopy indicated that extensive secondary structures associated with the folding of LYZ occurred, although such structures were only marginally protected from hydrogen/deuterium exchange.[26,27]

Spectral snapshots and a kinetic curve for in-gel LYZ folding are shown in Figures 4D and 5D, respectively. The kinetic curves acquired at different wavelengths could all be fit with a single exponential function and identical rate constants (Figure 5D, inset). This exponential decay can be ascribed to the formation of an I state that corresponds to the solution burst-phase I state because the spectrum at 3 min (Figure 4D) is very similar in shape and amplitude to that of the solution burst-phase I state.[24]

Activation Energies of I-State Formation. The activation energies (E_a) for formation of the I states were obtained from the temperature dependence of the rate constant for each protein. To confirm that the height of an activation barrier is not affected by encapsulation, temperature dependence of the formation of the CYT intermediate was measured for systems with gels aged for 6 or 48 h (Figure 6A). The slopes, which reflect the E_a values, are nearly identical for both plots, although the CYT folding rate is 2-fold slower in the gel aged 48 h than in the gel aged 6 h, suggesting that the deceleration is caused by entropic factors.

Arrhenius plots for the other four proteins are shown in Figure 6B, and the activation energies are summarized in Table 1. Although the E_a value for BLA is significantly greater than those of the other proteins, their E_a values are the same within the uncertainties of the measurements.

Table 1. Activation Energies of I-State Formation in Silica Gels

protein	E_a[a] (kJ/mol)
β-lactoglobulin (ELG)	16.8 ± 2.1[b]
tear lipocalin (HTL)	17.0 ± 4.6[b]
α-lactalbumin (BLA)	30.6 ± 5.2[b]
lysozyme (LYZ)	20.8 ± 7.3[c]
cytochrome *c* (CYT)	14.4 ± 6.9[c], 15.0 ± 3.1[d]

[a]Temperature range, 5−25 °C. [b]Gel aged for 2 h. [c]Gel aged for 6 h. [d]Gel aged for 48 h.

DISCUSSION

Burst-Phase Folding of ELG, BLA, LYZ, and HTL in a Silica Gel. This study revealed that the unresolved kinetic phases of the four proteins in solution consist of at least two kinetic processes in gel, one being a transition that occurs within the observation dead time (~5 s). To reconstruct the CD spectra of the in-gel burst phase species, the MRE values at various wavelengths were extrapolated back to zero time, and the resulting spectra are shown in Figure 4. For all four proteins, their burst-phase CD spectra are more negative than

dx.doi.org/10.1021/bi5003647 | *Biochemistry* 2014, 53, 3858−3866

are those of their U states in 6 M GdnHCl. The GdnHCl-induced unfolding equilibrium curves of ELG, BLA, and LYZ have been monitored by the MRE change at 222 nm.[20,25] The urea-induced equilibrium-unfolding curve of HTL was also monitored by the MRE change at 222 nm.[23] In all cases, the MRE increased linearly with increasing denaturant concentration after the cooperative transition had been completed and the linear increases were interpreted as shifts in the conformational ensembles of the U states that depended on the denaturant concentration. Assuming a linear dependence of MRE on the denaturant concentration, then by extrapolating to 0 M denaturant, the ellipticity of an unfolded protein in the absence of denaturant is obtained. This value is −6000 deg·cm^2/dmol for ELG,[20] −3000 deg·cm^2/dmol for HTL,[23] −4200 deg·cm^2/dmol for BLA,[25] and −3700 deg·cm^2/dmol for LYZ.[25] Although these values have large uncertainties because of the long extrapolations from narrow concentration ranges, they are similar to the MRE values found for the in-gel burst-phase MRE values at 222 nm (Figure 4). Therefore, the rapid spectral changes that occur within the dead time of our experiments might be a consequence of conformational shifts within the unfolded ensemble upon lowering the GdnHCl concentration (a U → U′ transition). Unfolded proteins in a concentrated denaturant solution (i.e., a good solvent) are highly expanded but become compact as the denaturant concentration is decreased (i.e., a poor solvent).[36] Therefore, changes in the MRE values during the proteins' burst phases in the gels may reflect, in part, a shift in the backbone conformational preferences from their unfolded states to their collapsed states upon lowering the GdnHCl concentration. The changes in MRE during the burst phases may also be a consequence of nonspecific burial of aromatic residues and disulfides in the collapsed state because the far-UV transitions of these residues can contribute substantially to the corresponding CD spectrum.[37−39]

Previously, Krantz et al.[40] raised a question about interpretation of solution burst-phase signal. They ascribed the solution burst-phase signal to the aggregation or contraction of U state upon dilution of denaturant. However, the observation that the in-gel I states are formed via single exponential kinetics and the in-gel I states correspond to the solution burst-phase I states strongly evidence that solution burst-phase signals of the four proteins investigated here reflect the formation of discrete intermediates.

E_a Barriers. The time-resolved CD changes upon formation of the in-gel I state for all of the proteins, except CYT, which were not resolvable for the solution experiments, exhibit single exponential kinetics. Such kinetics have been interpreted as reflecting a two-state cooperative, barrier-crossing process.[33,41] To evaluate the energy barriers between the U′ state and the I state for each of the proteins, we performed in-gel folding experiments between 5 and 25 °C and obtained E_a values from the corresponding Arrhenius plots (Figure 6, Table 1). The E_a value for the fastest resolved kinetic phase of CYT is 14−15 kJ/mol irrespective of the gel-aging time (Table 1). Using a continuous-flow mixing apparatus, for which the dead time was 45 μs, Shastry and Roder[33] found two fluorescent phases for CYT folding with rate constants of 17 000 s^{-1} and 2300 s^{-1} at pH 4.5 and 22 °C. They interpreted the first phase as polypeptide chain collapse and evaluated its E_a to be 30 kJ/mol. Under the same conditions, using a continuous-flow CD apparatus of which the earliest detectable time is ∼400 μs, Akiyama et al. found that the fastest measurable change in MRE occurred with a rate constant of 2300 s^{-1} in addition to the burst-phase change.[42] These results suggest that the burst-phase CD change may occur at an identical rate with the faster one observed by Shastry and Roder. Because the CD spectrum of the in-gel I state observed in this study is similar to the spectrum of an earliest intermediate observed in solution by Akiyama et al., the fastest resolvable kinetics in this study (Figure 3B) corresponds to the fastest one observed by Shastry and Roder. If this is the case, the E_a value we calculated (15 kJ/mol between 5 and 25 °C) may be compared with that obtained by Shastry and Roder in their solution study (30 kJ/mol between 10 and 29 °C). The difference between the two values may be a consequence of the presence or absence of the gel enclosure. It was also reported that the expansion kinetics induced by a laser temperature-jump (within several tens of nanoseconds), was accompanied by E_a values of 26−41 kJ/mol in the presence of 1.5 M GdnHCl between 17 and 43 °C,[41,43] which is also larger than the value obtained here. Nevertheless, this study showed that the α-helices are formed during the earliest kinetic phase. Previous studies discussed above used fluorescence observation and ascribed the fluorescent changes to a collapse or expansion of CYT.[33,41,43] Hagen showed that a barrierless diffusional process can give rise to kinetics that are practically indistinguishable from single exponential kinetics.[44] It has also been suggested that the viscosity of water has an Arrhenius-like temperature dependence near room temperature.[41] However, the results presented here and the previous study[14] suggest that α-helices are formed concurrent with fluorescence quenching. Therefore, the E_a for CYT probably, at least in part, reflects α-helical hydrogen bond formation.

To the best of our knowledge, we are the first to resolve the solution burst-phase events of ELG, HTL, BLA, and LYZ folding. For each protein, the solution burst phase could be resolved into two phases, an in-gel burst phase and a single measurable exponential relaxation phase for which the E_a values were between 16 and 31 kJ/mol (Table 1). Interestingly, the E_a values of ELG and HTL are nearly identical to each other despite the different secondary structure content in their I states (Figures 3A,B). The E_a values for ELG and HTL are also similar to those of CYT and LYZ, suggesting that secondary structure may not be a major determinant of E_a. Why formation of the BLA I state has a greater E_a value is not clear. Nevertheless, together with their single-exponential behaviors, the positive E_a values signify that formation of the early folding I states are barrier-crossing processes in the gels.

AUTHOR INFORMATION

Corresponding Author

*Masamichi Ikeguchi. E-mail: ikeguchi@soka.ac.jp. Phone: +81-426-91-9444.

Present Address

§S.T.: Department of Cell Physiology, The Jikei University School of Medicine, 3-25-8 Nishishinbashi, Minatoku, Tokyo 105-8461, Japan.

Notes

The authors declare no competing financial interest.

ACKNOWLEDGMENTS

The authors thank Prof. K Kuwajima for valuable comments on the manuscript.

■ ABBREVIATIONS

BLA, bovine α-lactalbumin; BLG, bovine β-lactoglobulin; CYT, horse heart cytochrome *c*; ELG, equine β-lactoglobulin; GdnHCl, guanidine hydrochloride; HTL, human tear lipocalin; LYZ, hen egg lysozyme; MRE, mean residue ellipticity; TMOS, tetramethylorthosilicate

■ REFERENCES

(1) Kuwajima, K. (1989) The molten globule state as a clue for understanding the folding and cooperativity of globular-protein structure. *Proteins 6*, 87−103.

(2) Ferguson, N., and Fersht, A. R. (2003) Early events in protein folding. *Curr. Opin. Struct. Biol. 13*, 75−81.

(3) Roder, H., Maki, K., and Cheng, H. (2006) Early events in protein folding explored by rapid mixing methods. *Chem. Rev. 106*, 1836−1861.

(4) Kathuria, S. V., Guo, L., Graceffa, R., Barrea, R., Nobrega, R. P., Matthews, C. R., Irving, T. C., and Bilsel, O. (2011) Minireview: Structural insights into early folding events using continuous-flow time-resolved small-angle X-ray scattering. *Biopolymers 95*, 550−558.

(5) Udgaonkar, J. B. (2013) Polypeptide chain collapse and protein folding. *Arch. Biochem. Biophys. 531*, 24−33.

(6) Eaton, W. A., Munoz, V., Thompson, P. A., Henry, E. R., and Hofrichter, J. (1998) Kinetics and dynamics of loops, α-helices, β-hairpins, and fast-folding proteins. *Acc. Chem. Res. 31*, 745−753.

(7) Gruebele, M., Sabelko, J., Ballew, R., and Ervin, J. (1998) Laser temperature jump induced protein refolding. *Acc. Chem. Res. 31*, 699−707.

(8) Ellerby, L. M., Nishida, C. R., Nishida, F., Yamanaka, S. A., Dunn, B., Valentine, J. S., and Zink, J. I. (1992) Encapsulation of proteins in transparent porous silicate glasses prepared by the sol-gel method. *Science 255*, 1113−1115.

(9) Shibayama, N., and Saigo, S. (1995) Fixation of the quaternary structures of human adult haemoglobin by encapsulation in transparent porous silica gels. *J. Mol. Biol. 251*, 203−209.

(10) Bettati, S., and Mozzarelli, A. (1997) T state hemoglobin binds oxygen noncooperatively with allosteric effects of protons, inositol hexaphosphate, and chloride. *J. Biol. Chem. 272*, 32050−32055.

(11) Shibayama, N., and Saigo, S. (1999) Kinetics of the allosteric transition in hemoglobin within silicate sol-gels. *J. Am. Chem. Soc. 121*, 444−445.

(12) Samuni, U., Navati, M. S., Juszczak, L. J., Dantsker, D., Yang, M., and Friedman, J. M. (2000) Unfolding and refolding of sol-gel encapsulated carbonmonoxymyoglobin: An orchestrated spectroscopic study of intermediates and kinetics. *J. Phys. Chem. B 104*, 10802−10813.

(13) Peterson, E. S., Leonard, E. F., Foulke, J. A., Oliff, M. C., Salisbury, R. D., and Kim, D. Y. (2008) Folding myoglobin within a sol-gel glass: protein folding constrained to a small volume. *Biophys. J. 95*, 322−332.

(14) Shibayama, N. (2008) Slow motion analysis of protein folding intermediates within wet silica gels. *Biochemistry 47*, 5784−5794.

(15) Shibayama, N. (2008) Circular dichroism study on the early folding events of β-lactoglobulin entrapped in wet silica gels. *FEBS Lett. 582*, 2668−2672.

(16) Eggers, D. K., and Valentine, J. S. (2001) Crowding and hydration effects on protein conformation: A study with sol-gel encapsulated proteins. *J. Mol. Biol. 314*, 911−922.

(17) Crupi, V., Majolino, D., Migliardo, P., and Venuti, V. (2002) Neutron scattering study and dynamic properties of hydrogen-bonded liquids in mesoscopic confinement. 1. The water case. *J. Phys. Chem. B 106*, 10884−10894.

(18) Milischuk, A. A., and Ladanyi, B. M. (2011) Structure and dynamics of water confined in silica nanopores. *J. Chem. Phys. 135*, 174709−174711.

(19) Sabelko, J., Ervin, J., and Gruebele, M. (1999) Observation of strange kinetics in protein folding. *Proc. Natl. Acad. Sci. U. S. A. 96*, 6031−6036.

(20) Fujiwara, K., Arai, M., Shimizu, A., Ikeguchi, M., Kuwajima, K., and Sugai, S. (1999) Folding-unfolding equilibrium and kinetics of equine β-lactoglobulin: Equivalence between the equilibrium molten globule state and a burst-phase folding intermediate. *Biochemistry 38*, 4455−4463.

(21) Kuwata, K., Shastry, R., Cheng, H., Hoshino, M., Batt, C. A., Goto, Y., and Roder, H. (2001) Structural and kinetic characterization of early folding events in β-lactoglobulin. *Nat. Struct. Biol. 8*, 151−155.

(22) Nakagawa, K., Tokushima, A., Fujiwara, K., and Ikeguchi, M. (2006) Proline scanning mutagenesis reveals non-native fold in the molten globule state of equine β-lactoglobulin. *Biochemistry 45*, 15468−15473.

(23) Tsukamoto, S., Yamashita, T., Yamada, Y., Fujiwara, K., Maki, K., Kuwajima, K., Matsumura, Y., Kihara, H., Tsuge, H., and Ikeguchi, M. (2009) Non-native α-helix formation is not necessary for folding of lipocalin: Comparison of burst-phase folding between tear lipocalin and β-lactoglobulin. *Proteins 76*, 226−236.

(24) Kuwajima, K., Hiraoka, Y., Ikeguchi, M., and Sugai, S. (1985) Comparison of the transient folding intermediates in lysozyme and α-lactalbumin. *Biochemistry 24*, 874−881.

(25) Ikeguchi, M., Kuwajima, K., Mitani, M., and Sugai, S. (1986) Evidence for identity between the equilibrium unfolding intermediate and a transient folding intermediate: a comparative study of the folding reactions of α-lactalbumin and lysozyme. *Biochemistry 25*, 6965−6972.

(26) Dobson, C. M., Evans, P. A., and Radford, S. E. (1994) Understanding how proteins fold: the lysozyme story so far. *Trends Biochem. Sci. 19*, 31−37.

(27) Matagne, A., and Dobson, C. M. (1998) The folding process of hen lysozyme: A perspective from the 'new view'. *Cell. Mol. Life Sci. 54*, 363−371.

(28) Forge, V., Wijesinha, R. T., Balbach, J., Brew, K., Robinson, C. V., Redfield, C., and Dobson, C. M. L. (1999) Rapid collapse and slow structural reorganisation during the refolding of bovine α-lactalbumin. *J. Mol. Biol. 288*, 673−688.

(29) Arai, M., and Kuwajima, K. (2000) Role of the molten globule state in protein folding. *Adv. Protein Chem. 53*, 209−282.

(30) Wijesinha-Bettoni, R., Dobson, C. M., and Redfield, C. (2001) Comparison of the denaturant-induced unfolding of the bovine and human α-lactalbumin molten globules. *J. Mol. Biol. 312*, 261−273.

(31) Arai, M., Ito, K., Inobe, T., Nakao, M., Maki, K., Kamagata, K., Kihara, H., Amemiya, Y., and Kuwajima, K. (2002) Fast compaction of α-lactalbumin during folding studied by stopped-flow X-ray scattering. *J. Mol. Biol. 321*, 121−132.

(32) Gohda, S., Shimizu, A., Ikeguchi, M., and Sugai, S. (1995) The superreactive disulfide bonds in α-lactalbumin and lysozyme. *J. Protein Chem. 14*, 731−737.

(33) Shastry, M. C., and Roder, H. (1998) Evidence for barrier-limited protein folding kinetics on the microsecond time scale. *Nat. Struct. Biol. 5*, 385−392.

(34) Ikeguchi, M., Kato, S., Shimizu, A., and Sugai, S. (1997) Molten globule state of equine β-lactoglobulin. *Proteins 27*, 567−575.

(35) Yamamoto, M., Nakagawa, K., Fujiwara, K., Shimizu, A., and Ikeguchi, M. (2011) A native disulfide stabilizes non-native helical structures in partially folded states of equine β-lactoglobulin. *Biochemistry 50*, 10590−10597.

(36) Sherman, E., and Haran, G. (2006) Coil-globule transition in the denatured state of a small protein. *Proc. Natl. Acad. Sci. U. S. A. 103*, 11539−11543.

(37) Chakrabartty, A., Kortemme, T., Padmanabhan, S., and Baldwin, R. L. (1993) Aromatic side-chain contribution to far-ultraviolet circular dichroism of helical peptides and its effect on measurement of helix propensities. *Biochemistry 32*, 5560−5565.

(38) Vuilleumier, S., Sancho, J., Loewenthal, R., and Fersht, A. R. (1993) Circular dichroism studies of barnase and its mutants: Characterization of the contribution of aromatic side chains. *Biochemistry 32*, 10303−10313.

(39) Sreerama, N., and Woody, R. W. (2004) Computation and analysis of protein circular dichroism spectra. *Methods Enzymol. 383*, 318−351.

(40) Krantz, B. A., Mayne, L., Rumbley, J., Englander, S. W., and Sosnick, T. R. (2002) Fast and slow intermediate accumulation and the initial barrier mechanism in protein folding. *J. Mol. Biol. 324*, 359−371.
(41) Hagen, S. J., and Eaton, W. A. (2000) Two-state expansion and collapse of a polypeptide. *J. Mol. Biol. 301*, 1019−1027.
(42) Akiyama, S., Takahashi, S., Ishimori, K., and Morishima, I. (2000) Stepwise formation of α-helices during cytochrome c folding. *Nat. Struct. Biol. 7*, 514−520.
(43) Qiu, L., Zachariah, C., and Hagen, S. J. (2003) Fast Chain Contraction during Protein Folding: ″Foldability″ and Collapse Dynamics. *Phys. Rev. Lett. 90*, No. 168103.
(44) Hagen, S. J. (2003) Exponential decay kinetics in "downhill" protein folding. *Proteins 50*, 1−4.